European Geosciences Union General Assembly 2013, Vienna, Austria, 7-12 April 2013, Session NH1.6/B325: Flood Risk and Uncertainty Vol. 15, EGU2013-10283-2

Alternative methods in floodplain hydraulic simulation – Experiences and perspectives

Pagana V.[1], Tegos A.[1,2], Dimitriadis P.[1], Koukouvinos A.[1], Panagopoulos P. D.[2], Mamassis N.[1]

[1] Department of Water Resources and Environmental Engineering, National Technical University of Athens

[2] ECOS Consulting S.A.

1. Abstract

Floods can simply be defined as the physical phenomena, during which an initially dry land area is covered by water. Floods are normally caused by climatic changes, while their evolution depends mainly on geomorphologic factors, such as soil stability, vegetation cover, as well as the geometrical characteristics of the river basin. To prevent floods' consequences, we have to study the hydraulic behavior of all the basins. Here, the study is focused on the upstream part of the Rafina basin, located in the east of Athens (Greece). Particularly, a hydraulic simulation is accomplished via the one-dimensional HEC-RAS and the quasi-two-dimensional LISFLOOD-FP and FLO-2D models. Additionally, a sensitivity analysis is carried out to investigate the effects of the floodplain and river roughness coefficients on the flood inundation in conjunction with a modern probabilistic view. Finally, a comparison between the three models is made regarding the simulated maximum water depth and maximum flow velocity.

2. Introduction

Rafina catchment is located in the greater southeast Mesogeia region in eastern Attica, Greece. This area covers 127 km^2 and geographically extends east of Ymittos mountain to the coastline of Evoikos Gulf. Rafina basin is covered by different and often conflicting land uses. More specifically, it includes forests (~30%), arable soils and grasslands (~50%) mainly located upstream and urban cells (~20%) located downstream. The mean altitude of this region is 227 m approximately. The max value is 909 m and the mean one is 0m. Regarding the ground slope, it ranges from 0% to 37.8%. The mean value is calculated to 7.5%. Increased slopes refer mainly to the upstream parts of the area and are clustered at its north part. Regarding the hydrometeorological regime, Attica has a typical Mediterranean climate. The mean annual precipitation is approximately 400 mm, while snowfall is rare.

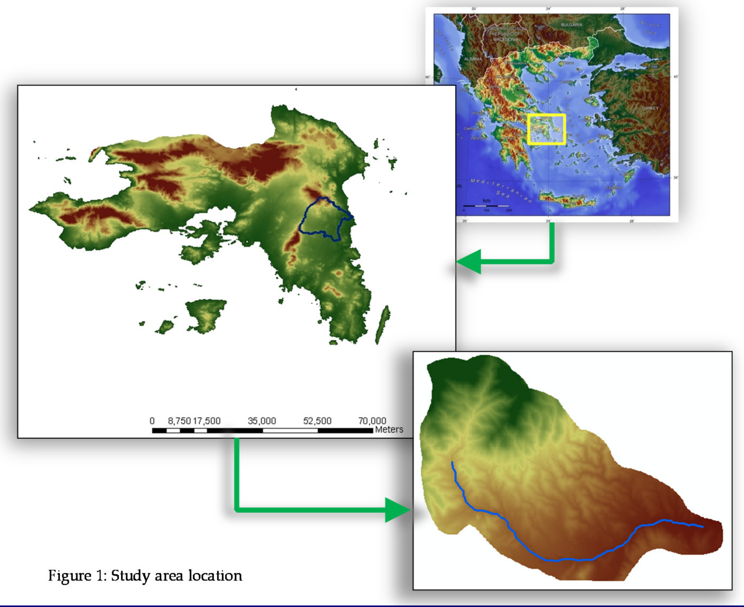

Figure 1: Study area location

3. Input data

In this section, collected data are presented. These data are topographic, hydrologic and hydraulic. Concerning the topography, a digital elevation model with pixel size 5 m and a land use map are used. The land use map is necessary for the estimation of Manning value. Table 1 shows the land uses and the respective Manning coefficient value. A real photo of the area justifies these values. Concerning the hydrologic data, ombrian curves (Equation 1) are used for the estimation of rainfall hyetograph. These data are processing through HEC-HMS and they give the flood hydrograph (Figure 3) which presents a peak = 244.8 m^3/s. Finally the data that are used in hydraulic simulation are, 7 km of total river (12 m width), 11 cross sections (500 m width), manning values and boundary conditions.

• Ombrian Curves (Kifissos Basin)

$$i(d,T) = \frac{260\,(T^{0.15} - 0.61)}{\left(1 + d/0.17\right)^{0.77}}, \quad (1)$$ (Koutsoyiannis et a.l.,2010)

i: rainfall intensity (mm/h)
d: time step, 15 min
T: return period, 500 years

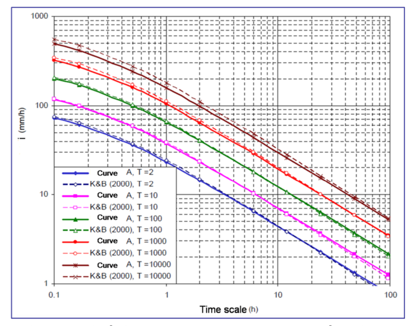

Figure 2: Ombrian curves (Koutsoyiannis et al., 2010)

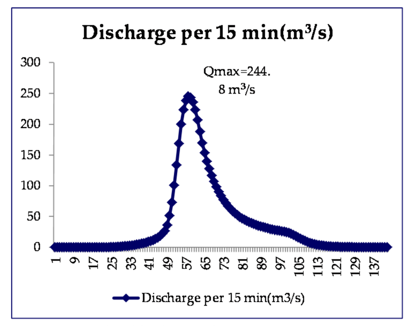

Figure 3: Flood hydrograph, time step 15 min

• Manning coefficient

LU Code	n Value	Description
122	0.015	Gravel and stones
311	0.04	Broaded- leaved forest

Table 1: land uses and respective n coefficient

Figure 4: On site photograph of the river.

Notation: Based on the 'on site' picture Manning's coefficient choice is justified by observing the land uses close to the river: $\mathbf{n_{channel} = 0.015\ m^{-1/3}s}$, $\mathbf{n_{banks} = 0.04\ m^{-1/3}s}$

4. Hydraulic models interface

✓HEC - RAS

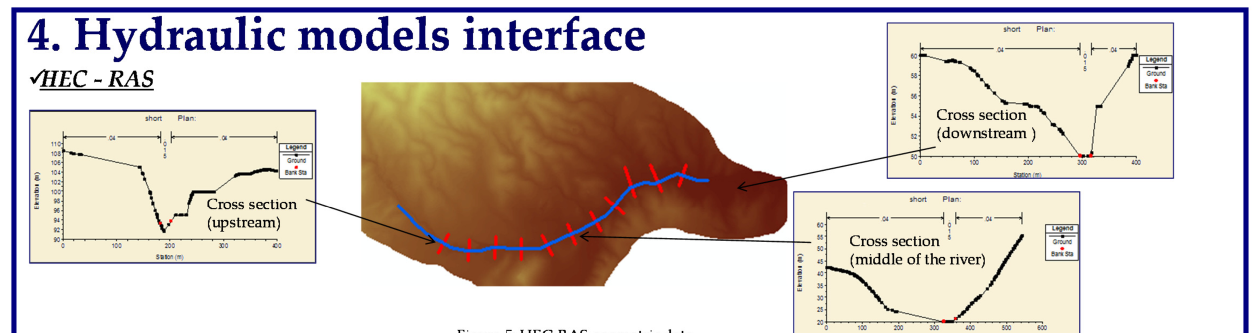

Figure 5: HEC-RAS geometric data

✓FLO-2D

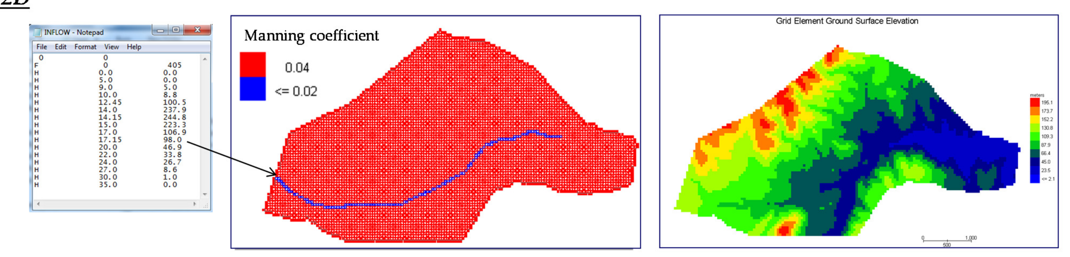

Figure 6: FLO-2D inflow file (left) and Manning coefficient (middle) and elevation (right) gridded map.

✓LISFLOOD-FP

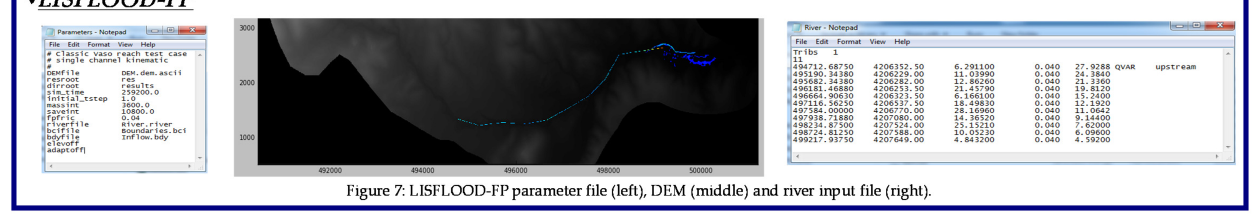

Figure 7: LISFLOOD-FP parameter file (left), DEM (middle) and river input file (right).

5a. HEC-RAS simulations

General information
- http://www.hec.usace.army.mil/software/hec-ras/
- Open access software
- 1- dimensional hydraulic model
  - ✓Steady flow analysis
  - ✓Unsteady flow analysis — Saint Venant Equations

Input data
- ✓Geometric file ⟶ Manning coefficient
  - **n= 0.015** central channel, **n= 0.004** banks
- ✓Flow data ⟶ Flood Hydrograph (with 10 min interval)
- ✓Boundary Conditions
  - Flood Hydrograph (upstream)
  - Normal depth = 0.18 (downstream)

Output data (11 cross-sections)
- ✓Max channel depth (m)
- ✓Max velocity (m/s)
- ✓Discharge (m^3/s)

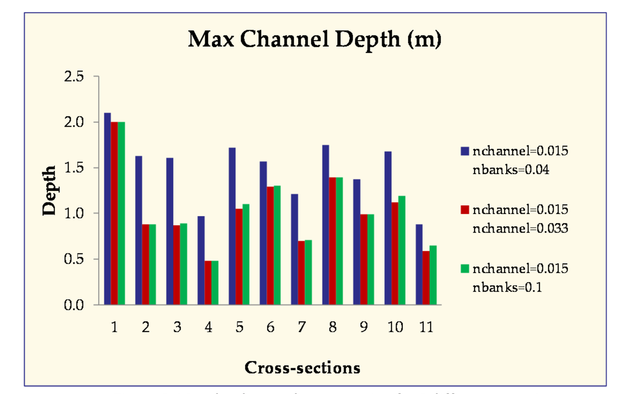

Figure 8: Max depth to each cross section for 3 different scenarios

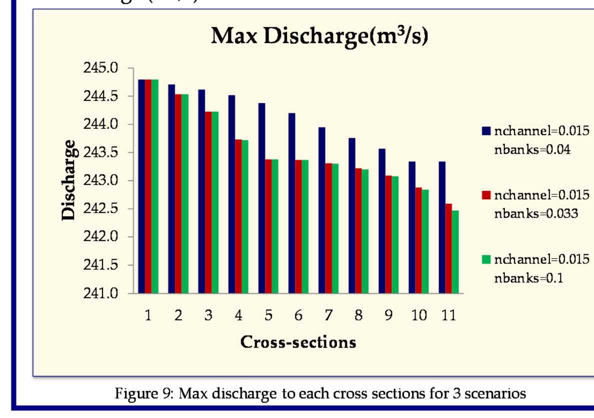

Figure 9: Max discharge to each cross sections for 3 scenarios

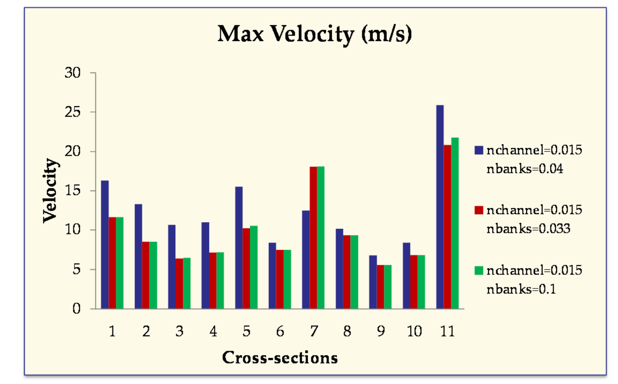

Figure 10: Max velocity to each cross sections for 3 scenarios

5b. FLO-2D simulations

General information
- https://www.flo-2d.com/
- Open access software
- Quasi 2-dimensional grid-based hydraulic model (dynamic wave)

Output data (11 grid cells)
- ✓Max channel depth (m)
- ✓Max velocity (m/s)

Input data
- ✓Geometric file ⟶ Manning coefficient
  - 6 scenarios (see Table 2 on the right)
- ✓Flow data (input hydrograph)
- ✓Boundary Conditions
  - Flood Hydrograph (upstream)
- ✓No channel input
- ✓Grid size 50 m

Scenarios	Manning Banks	Manning River
1	0.1	
2	0.04	
3	0.033	
4	0.1	0.015
5	0.04	0.015
6	0.033	0.015

Table 2: FLO-2D simulation scenarios

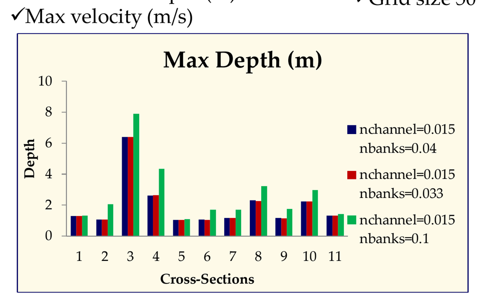

Figure 11: Max depth to each grid cell for $n_{channel} \# n_{banks}$

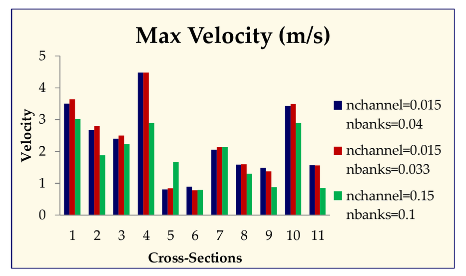

Figure 12: Max velocity to each grid cell for $n_{channel} \# n_{banks}$

Concerning the 3 last scenarios the max channel depth exhibits an increase in the case where the Manning coefficient at the banks is **0.1**. In the two other cases the max depth exhibits the same behavior.

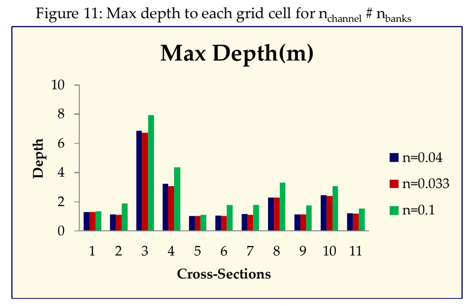

Figure 13: Max depth to each grid cell for $n_{channel}=n_{banks}$

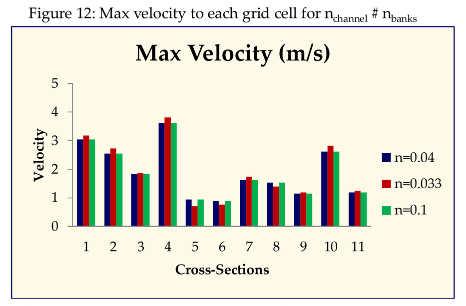

Figure14: Max velocity to each grid cell for $n_{channel}=n_{banks}$

Concerning the scenarios where the Manning coefficient remains the same (channel and banks), the largest max depth is estimated with n=0.1. The max velocities do not exhibit major differences.

5c. LISFLOOD-FP simulations

General information
- http://www.bris.ac.uk/geography/research/hydrology/models/lisflood
- Open access software
- Quasi 2-dimensional grid-based hydraulic model (kinematic wave)
- Considers rectangular river cross sections

Output data (11 grid cells)
- ✓Max channel depth (m)

Input data
- ✓Geometric file ⟶ Manning coefficient
  - 6 scenarios (see Table 2)
- ✓Flow data (input hydrograph)
- ✓Boundary Conditions
  - Flood Hydrograph (upstream)
- ✓Grid size 5 m

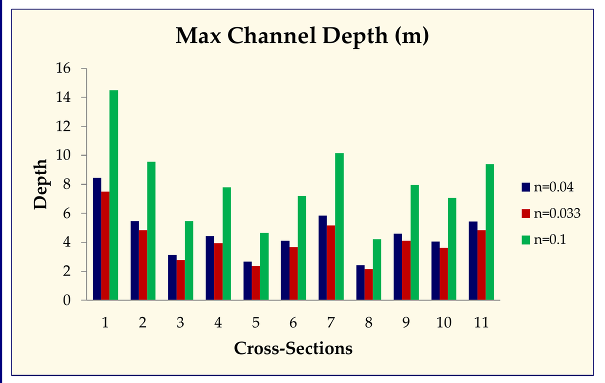

Figure15: Max depth to each grid cell for $n_{channel}=n_{banks}$

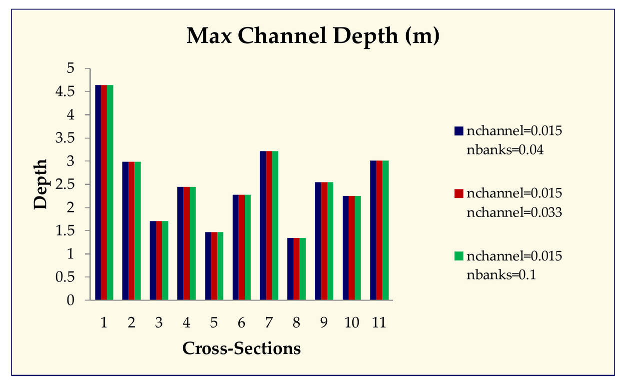

Figure16: Max depth to each grid cell for $n_{channel} \# n_{banks}$

Max channel depth exhibits differences in the case where the Manning coefficient is considered the same both in channel and banks. However, in the case where the Manning coefficient is changed only in the banks, the max channel depth remains invariable.

5d. Comparison of the 3 models

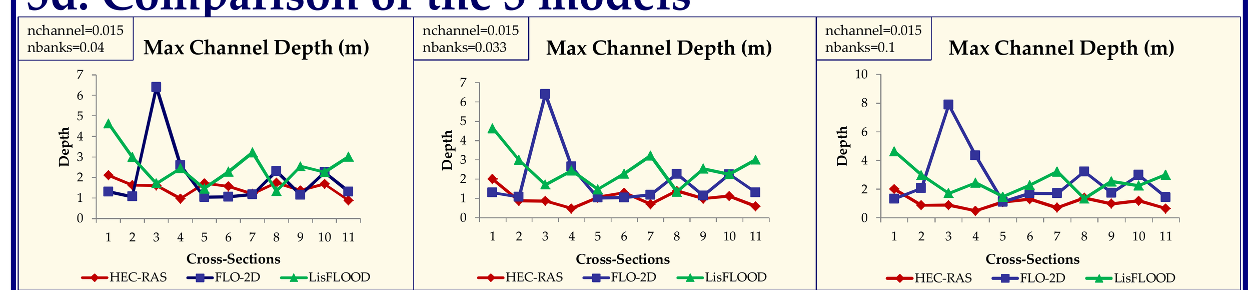

Figure17: Comparison of max depth to each cross sections/grid cell for 3 different scenarios.

It is observed that the max depths exhibit differences among the 3 models. Particularly, FLO-2D gives larger values in the upstream area, probably due to the absence of channel modeling. Concerning the downstream area's water depths, their differences range from 0.2 to 2 m. The min values mostly belong to the HEC-RAS simulations. Also, it seems that the results of LISFLOOD-FP remain mostly invariable for all the scenarios.

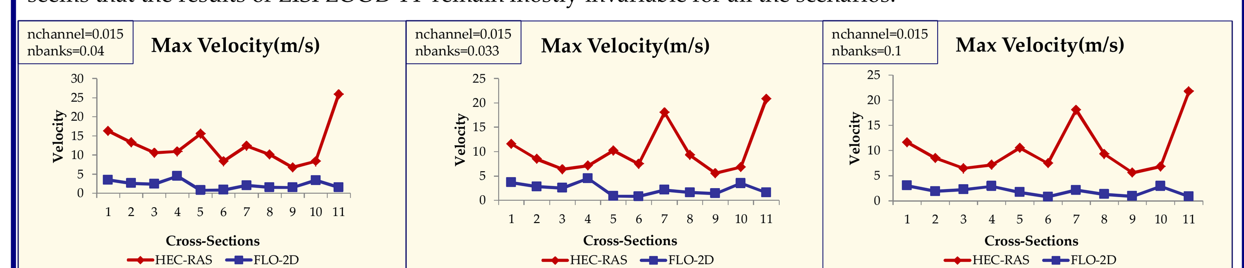

Figure18: Comparison of max velocity to each cross section/grid cell for 3 different scenarios.

Finally, it can be observed from the figures above, that the HEC-RAS simulations exhibit higher max velocity than the FLO-2D ones, again probably due to the absence of channel modeling in the FLO-2D, resulting in smaller discharge values within the floodplain.

6. Sensitivity analysis of the 3 models

A sensitivity analysis is made in order to introduce a probabilistic view of the flood mapping, necessary when simulating a flood event (i.e. Baltassare et al. 2010). The tested parameters are the river and floodplains Manning's coefficients varying uniformly from 0.01 (corresponding to neat surface) to 0.1 m$^{-1/3}$s (corresponding to very weedy reaches), as well as the river's discharge varying uniformly from 250 m^3/s (corresponding to a 500 years return period) to 1000 m^3/s (corresponding to a 100000 years return period). Also, a steady flow condition is chosen and 100 simulations are made for each model. The recorded parameter is chosen as the water depth which is a common output in all 3 models and the recorded locations are chosen as the 11 cross sections (for HEC-RAS) or grid cells (for LISFLOOD-FP and FLO-2D). The 5 m x 5 m DEM analysis is chosen for HEC-RAS and LISFLOOD-FP and the 50 m x 50 m DEM analysis for FLO-2D.

	Cross section	1	2	3	4	5	6	7	8	9	10	11
HEC-RAS	Min	1.92	2.09	1.76	1.38	1.59	1.60	1.47	2.72	1.30	1.43	1.13
	Max	5.95	6.04	6.39	4.10	4.53	5.45	6.15	6.47	4.96	4.59	4.12
	Average	3.54	4.06	3.48	2.70	2.75	2.88	3.94	4.13	2.63	2.87	2.36
	Standard deviation	0.98	1.10	1.02	0.77	0.64	0.86	1.03	0.72	1.07	0.73	0.73
LISFLOOD	Min	6.31	4.07	2.34	3.34	2.01	3.12	4.42	1.84	3.50	3.11	4.16
	Max	23.05	20.33	11.84	16.95	10.17	15.84	22.43	9.33	17.77	15.77	21.10
	Average	15.85	11.67	6.70	9.60	5.76	8.97	12.70	5.28	10.06	8.92	11.94
	Standard deviation	4.23	4.12	2.37	3.40	2.04	3.18	4.50	1.87	3.56	3.16	4.23
FLO-2D	Min	1.35	1.18	6.74	2.93	1.08	1.05	1.15	2.30	1.16	2.43	1.25
	Max	2.79	4.79	11.07	6.78	2.45	3.75	3.89	5.60	3.27	4.43	2.42
	Average	1.94	3.09	9.36	5.08	1.58	2.34	2.49	4.08	2.10	3.44	1.76
	Standard deviation	0.37	0.95	1.02	0.84	0.39	0.75	0.71	0.81	0.54	0.47	0.31

Table 3: Overall results from the sensitivity analysis of the water depth at each cross section.

The simulation time for the 100 simulations is estimated to 30 min for HEC-RAS, 8 hrs for LISFLOOD-FP and 4 hrs for FLO-2D.

It can be observed from Table 3 on the left, that the smallest average as well as standard deviation values come from the FLO-2D simulations, probably due to the larger cell size. Also, it can be seen that HEC-RAS and LSIFLOOD-FP output water depths differ a lot, probably to the simplified geometry (of the rectangular cross section) of LISFLOOD-FP.

It seems that in cases where the river's area is large in its length but small in its width (thus, a small grid size must be applied), also, where is comparable to the floodplain's one (i.e. narrow topographies, small flood events) and the geometry of its cross sections differ a lot from a rectangular one (like in this study), HEC-RAS better represents the flood routing than the other two models examined. More information concerning the sensitivity analysis for each model separately can be viewed in the next sections.

7a. HEC-RAS sensitivity analysis

The main conclusion of this analysis is that HEC-RAS simulations seem to be much affective by the floodplain Manning coefficient rather than the river's one. This can be justified from Figure 19 which exhibits a water depth increasing behavior with both discharge and floodplain Manning coefficient; and from Figure 21 which exhibits the small sensitivity in the river roughness. This is a rational observation considering the 1d nature of HEC-RAS. Moreover, Figure 20 shows the water depth cumulative distribution functions of certain cross sections where the expected conclusion that they all should be close to a Normal one, based on the central limit theorem, is justified.

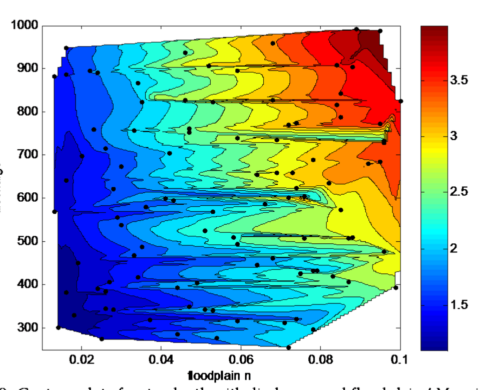

Figure 19: Contour plot of water depth with discharge and floodplains' Manning coefficient at the 8th cross section from sensitivity analysis' simulations.

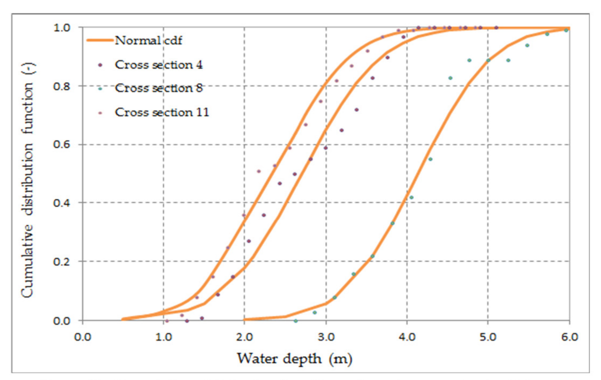

Figure 20: Cumulative distribution functions of maximum water depth from sensitivity analysis' simulations

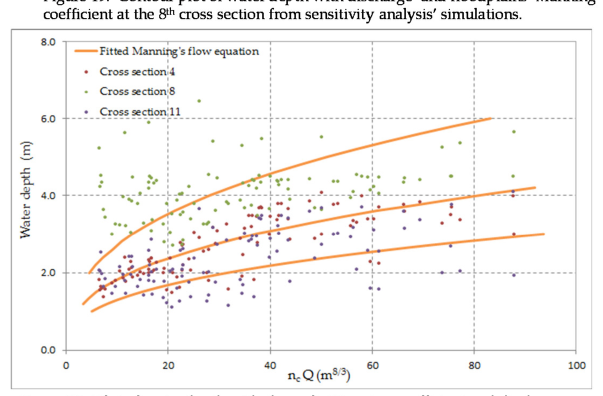

Figure 21: Plot of water depth with channel's Manning coefficient and discharge from sensitivity analysis' simulations.

7b. LISFLOOD-FP sensitivity analysis

The main conclusion of this analysis is that LISFLOOD-FP simulations seem to be much affective by the river Manning coefficient rather than the floodplain's one. This can be justified from Figure 22 which exhibits a water depth increasing behavior with both discharge and river Manning coefficient; and from Figure 24 which exhibits the infinitesimal sensitivity in the floodplain roughness. This is a rational observation considering the 2d nature of LISFLOOD-FP (e.g. see similar conclusions in Cunge et al., 1980 and Hunter et al., 2005). Moreover, Figure 23 shows the water depth cumulative distribution functions again well approximate the Normal one.

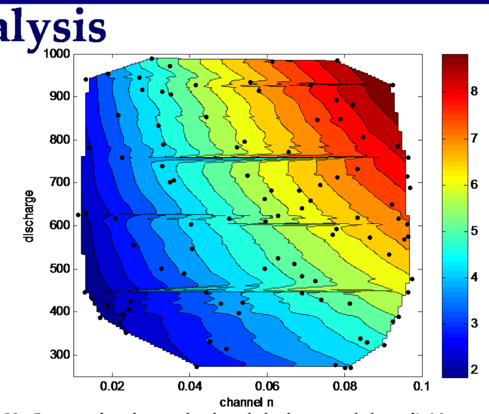

Figure 22: Contour plot of water depth with discharge and channel's Manning coefficient at the 8th cross section from sensitivity analysis' simulations.

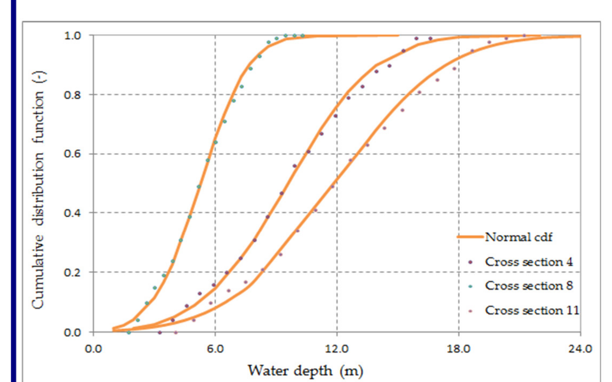

Figure 23: Cumulative distribution functions of maximum water depth from sensitivity analysis' simulations.

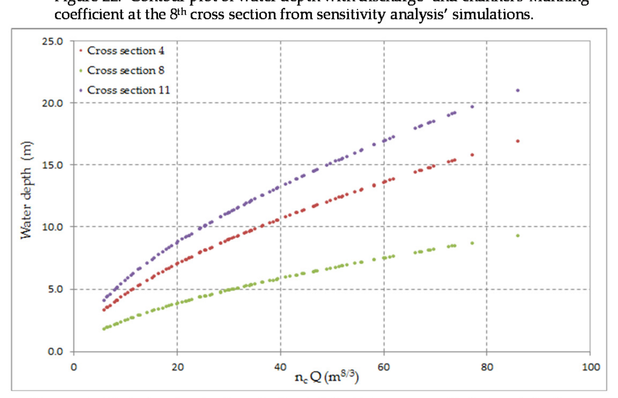

Figure 24: Plot of water depth with floodplains' Manning coefficient and discharge from sensitivity analysis' simulations.

7c. FLO-2D sensitivity analysis

The main conclusion of this analysis is that FLO-2D simulations seem to be much affective by the floodplain Manning coefficient rather than the river's one. This can be justified from Figure 25 which exhibits a water depth increasing behavior with both discharge and floodplain Manning coefficient; and from Figure 27 which exhibits the small sensitivity in the river roughness. This is not a rational observation considering the 2d nature of FLO-2D but it can be justified by the fact that the simulations are made without modeling the channel and also, with a large grid cell size which in most of the cases oversubscribe the simulated flood. Moreover, Figure 26 shows the water depth cumulative distribution functions which again well approximate the Normal one.

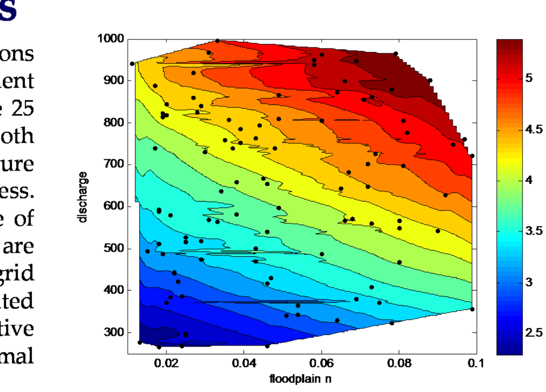

Figure 25: Contour plot of water depth with discharge and floodplains' Manning coefficient at the 8th cross section from sensitivity analysis' simulations.

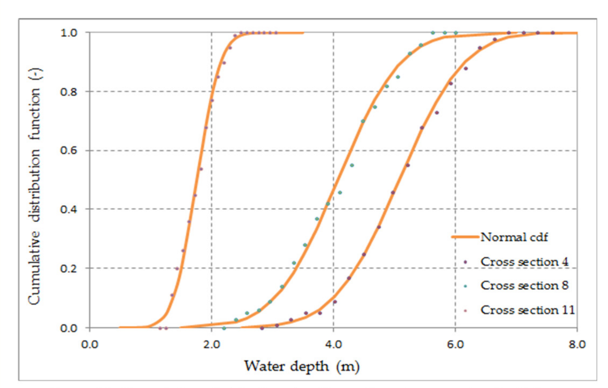

Figure 26: Cumulative distribution functions of maximum water depth from sensitivity analysis' simulations

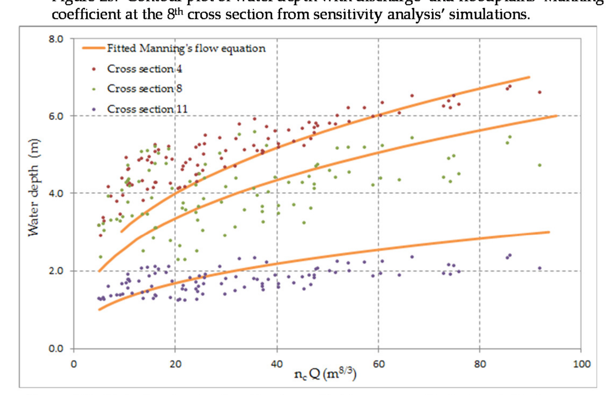

Figure 27: Plot of water depth with channel's Manning coefficient and discharge from sensitivity analysis' simulations.

8. Conclusions

Based on this study, it can be concluded that:
- HEC-RAS is not suggested for simulation in unsteady flow conditions. In the current study, to successfully run the model (i.e. without errors and warnings), it is necessary to interpolate the cross sections up to 0.5 m in some cases. Also, it is worth to refer that HEC-RAS often does not run successfully when the same Manning coefficient is applied in both channel and banks. Additionally, HEC-RAS interface often does not help when small changes to input data must be made (e.g. to change the Manning coefficient in all of the cross-sections at once). Nevertheless, HEC-RAS has been proved very powerful in steady flow conditions, especially in the case of narrow and steep rivers. From the three models tested, HEC-RAS seems to better represent the flood routing without the disadvantage of the simplified geometry of LISFLOOD-FP and the large cell size of FLO-2D.
- Concerning the sensitivity analysis, HEC-RAS is highly affected by changing floodplain Manning coefficient. Moreover, the sensitivity analysis of FLO-2D has the same behavior with HEC-RAS. This can be justified by the fact that there is no channel in the model. Also the grid cell size is big enough, so the total flow is concentrated in one cell. By contrast, LISFLOOD-FP is very sensitive to the changes of river's Manning coefficient.
- Also, it seems that all of the cumulative distribution functions of the water depth well approximate the Normal one.
- Finally, for future study, it is worth considering the uncertainty of other factors such as the quality of the DEM and the derivation of the ombrian curves.

References

- Baldassare Di G., Schumann G., Bates P.D., Freer J.E. and Keith Beven J.K., *Flood-plain mapping: a critical discussion of deterministic and probabilistic approaches*, Hydrological Sciences Journal, 55:3, 364-376, 2010.
- Bruner G., *HEC-RAS, river analysis system user's manual*, US Army corps of Engineers, Hydrologic engineering center, 2008a.
- Bruner G., *HEC-RAS, river analysis system hydraulic reference manual*, US Army corps of Engineers, Hydrologic engineering center, 2008b.
- Cameron T., Ackerman P.E., *HEC-GeoRAS, GIS tools for support of HEC-RAS using ArcGIS*, 2011.
- Cunge J.A., Holly F.M. Jr. and Verwey A., *Practical aspects of computational river hydraulics*, Pitman, London, 420pp, 1980.
- Hunter N.M., Horritt M.S., Bates P.D., Wilson M.D. and Werner M.G.F., *An adaptive time step solution for raster-based storage cell modelling of floodplain inundation*, Advances in Water Resources, 28(9), 975-991, 2005.
- Koutsoyiannis D., Y. Markonis, A. Koukouvinos, S.M. Papalexiou, N. Mamassis, and P. Dimitriadis, Hydrological study of severe rainfall in the Kephisos basin, Greece, *Study of the management of Kephisos*, Commissioner: General Secretariat of Public Works – Ministry of Environment, Planning and Public Works, Contractors: Exarhou Nikolopoulos Bensasson, Denco, G. Karavokiris, et al., 154 pages, Athens, 2010
- Pagana V., *Elaboration of flood inundation maps in Rafina basin*, Master Thesis, Inter-Departmental Postgraduate Course Water Resources Science and Technology, National Technical University of Athens (in Greek), 2012. http://itia.ntua.gr/en/docinfo/1213/
- Papathanasiou C., Makropoulos C. and Mimikou M., *The Hydrological Observatory of Athens: a state-of-the-art network for the assessment of the hydrometeorological regime of Attica*, Proc. 13th International Conference on Environmental Science and Technology, 5-7 September, Athens, Greece (full paper submitted and currently under review), 2013.